land

MDPI

Article

Potential Reduction of Spatiotemporal Patterns of Water and Wind Erosion with Conservation Tillage in Northeast China

Fahui Jiang [1], Xinhua Peng [1,2,*], Qinglin Li [3], Yongqi Qian [3] and Zhongbin Zhang [2,3]

[1] Key Laboratory of Agricultural Resources and Ecology in Poyang Lake Watershed of Ministry of Agriculture and Rural Affairs in China, Jiangxi Agricultural University, Nanchang 330045, China; fhjiangss@gmail.com
[2] Institute of Agricultural Resources and Regional Planning, Chinese Academy of Agricultural Sciences, Beijing 100081, China; zbzhang@issas.ac.cn
[3] State Key Laboratory of Soil and Sustainable Agriculture, Institute of Soil Science, Chinese Academy of Sciences, Nanjing 210008, China; qlli@issas.ac.cn (Q.L.); yqqian@issas.ac.cn (Y.Q.)
* Correspondence: pengxinhua@caas.cn

Abstract: Conservational tillage (NT) is widely recognized globally for its efficacy in mitigating soil loss due to wind and water erosion. However, a systematic large-scale estimate of NT's impact on soil loss reduction in Northeast, China's primary granary, remains absent. This study aimed to investigate the spatial and temporal variability of soil erosion under NT compared to conventional tillage (CT) in the black soil region and to analyze the underlying mechanisms driving these erosions. The Revised Universal Soil Loss Equation (RUSLE) and the Revised Wind Erosion Equation (RWEQ) models were employed, incorporating previously published plot/watershed data to estimate the potential reduction of water and wind erosion by NT in this region. Results indicated that under CT practices, water- and wind-induced soil losses were widely distributed in the arable land of Northeast China, with intensities of 2603 t km^{-2} a^{-1} and 34 t km^{-2} a^{-1}, respectively. Furthermore, the erosive processes of water and wind erosion were significantly reduced by 56.4% and 91.8%, respectively, under NT practices compared to CT. The highest efficiency in soil conservation using NT was observed in the mountainous regions such as the Changbai Mountains and Greater Khingan Mountains, where water erosion was primarily driven by cropland slopes and wind erosion was driven by the wind speed. Conversely, the largest areas of severe erosion were observed in the Songnen Plain, primarily due to the significant proportion of arable land in this region. In the plain regions, water-induced soil loss was primarily influenced by precipitation, with light and higher levels of erosion occurring more frequently on long gentle slopes (0–3°) than on higher slope areas (3–5°). In the temporal dimension, soil loss induced by water and wind erosion ceased during the winter under both tillage systems due to snow cover and water freezing in the soil combined with the extremely cold climate. Substantial reductions were observed under NT from spring to autumn compared to CT. Ultimately, the temporal and spatial variations of soil loss under CT and NT practices were established from 2010 to 2018 and then projected onto a cropland map of Northeast China. Based on this analysis, NT is recommended as most suitable practice in the southern regions of Northeast China for maintaining soil health and crop yield production, while its suitability decreases in the northern and eastern regions.

Keywords: no tillage; wind erosion; water erosion; soil erosion; conservation tillage

Citation: Jiang, F.; Peng, X.; Li, Q.; Qian, Y.; Zhang, Z. Potential Reduction of Spatiotemporal Patterns of Water and Wind Erosion with Conservation Tillage in Northeast China. *Land* **2024**, *13*, 1219. https://doi.org/10.3390/land13081219

Academic Editor: Zhi-Hua Shi

Received: 7 July 2024
Revised: 22 July 2024
Accepted: 2 August 2024
Published: 6 August 2024

1. Introduction

Soil erosion, a serious global issue, results in annual soil displacements of approximately 3590 and 58.3 billion tons by water and wind, respectively [1,2]. This erosion process leads to soil fertility loss, decreased productivity, increased flooding, and air pollution, posing significant threats to socio-ecological sustainability [3,4]. China's vast drylands, the world's largest, are significantly influenced by water and wind erosion, affecting 37.27%

and 34.39% of these regions, respectively [5,6]. Specifically, in the Northeast Plain of China, the nation's primary granary and the world's fourth-largest region of black soil (Mollisols), soil degradation due to wind and water erosion presents a significant threat to soil health, national food security, and agricultural sustainability. The multi-year average soil water erosion modulus and amount were estimated at 1.52 t ha^{-1} and 1.88 × 10^8 t, respectively, from 2000 to 2020 across Northeast China [7]. Similarly, the estimated values of wind erosion were 1.13 t ha^{-1} and 1.4 × 10^8 t during the same period [7]. These erosional processes have led to a significant depletion of fertile black soil thickness, with a mean erosion rate of 2.22 mm/a, which would result in complete erosion in approximately 113 years [8]. Consequently, compared with forest, grassland, wetland, and urban land, soil erosion were observed to be more severe in the cropland in the black soil region in the Northeast China. Therefore, it is urgent need to develop sustainable soil management strategies to mitigate soil erosion while maintaining black soil thickness in this region.

However, soil erosion in the arable lands of Northeast China has been exacerbated by traditional tillage practices, including autumn plowing, deep ploughing, rotary tillage, and ridge tillage [1,9]. Annually, several tillage practices are carried out on the arable land before planting. Soil clods are often crushed into smaller pieces, and soil roughness is reduced due to mechanical modifications with rotary tillers or moldboard plows, resulting in a loosened soil structure [9]. The crop straw and residue are frequently collected and used for fodder or fuel or sometimes buried in the field under traditional agriculture. Soil organic carbon is therefore significantly decreased with the duration of traditional tillage [10]. Consequently, sheet erosion is likely to increase under traditional tillage due to the loosened and bare soil surface [11]. Conservation tillage, i.e., no tillage with straw mulching (NT), is widely utilized to mitigate soil loss from wind and water erosion on a global scale [1]. Several studies have demonstrated the positive effects of NT practices on Northeast China's soil erosions. For instance, Zhang et al. [12] found a reduction in runoff by 71% to 98% and sediment loss by 89% to 99% under conservation tillage compared to conventional tillage (CT) in Hailun City. Wang et al. [13] documented an 82.6–85.5% decrease in runoff and an 87.9–91.5% reduction in soil erosion under NT compared to CT at the Lishu station. Jia et al. [14] and Chen et al. [15] demonstrated a reduction in soil wind erosion under NT in Changchun and Hailun. However, current studies in Northeast China primarily focus on plot monitoring or small watersheds, necessitating caution when advocating for widespread adoption. These studies do not provide a comprehensive understanding of soil erosion reduction across different regions and scales. Additionally, the suitability range of NT practices in the black soil region of Northeast China remains underexplored. Therefore, a systematic and large-scale estimate of the reduction in soil loss attributed to NT in Northeast China is essential. This research aims to fill these gaps by providing a comprehensive assessment of NT's effectiveness in mitigating soil erosion across various spatial and temporal scales.

The models of soil erosion predicting are invaluable tools for assessing the potential impact of NT and CT on regional scale. Various models have been developed. For instance, the Water Erosion Prediction Project (WEPP) is designed to simulate continuous and spatial changes in land use and soil properties across different slope and watershed scales [16,17]. The Limburg Soil Erosion Model (LISEM) operates on individual erodible-rainfall events to simulate soil loss at a watershed scale [18]. Nevertheless, obtaining the model's input indicators requires intensive field monitoring, posing a significant challenge. The European Soil Erosion Model (EUROSEM) is a highly accurate soil water erosion model capable of simulating sediment, runoff, and storm hydrographs in European contexts [19]. However, its applicability in Northeast China requires parameter adjustments to account for local soil and climate properties. In contrast, the Reversed Universal Soil Loss Equation (RUSLE) from America is the most widely used worldwide for assessing water erosion due to its robustness, ease of application, and adaptability to various geographic and climatic conditions [20]. In Northeast China, Zhang et al. [21] refined the RUSLE model using numerical data from 31 runoff test areas, 9 years of monitoring, and information from

20 weather stations. This refinement achieved a high accuracy of 0.9 in matching prediction data with measured data, demonstrating its reliability and effectiveness in the region. For wind erosion, the enhanced version of the Revised Wind Erosion Equation (RWEQ), derived from the Wind Erosion Equation (WEQ), is the most frequently used model in mainland China compared to others such as the Wind Erosion Prediction System (WEPS), Texas Erosion Analysis Model (TEAM), Wind Erosion Stochastic Simulator (WESS), Wind Erosion on European Light Soils (WEELS), Wind Erosion Assessment Model (WEAM), and the Integrated Wind Erosion Modelling System (IWEMS) [22]. In Northeast China, the RWEQ model has been shown to effectively predict wind erosion rates, making it suitable for assessing the wind erosion potential in the black soil zone due to its ability to account for the complex interactions among soil, vegetation, and climatic factors influencing wind erosion [2,3]. Therefore, the RUSLE and RWEQ models were selected to estimate the soil loss induced by water and wind erosion in the present study.

In the RUSLE/RWEQ modelling approach, both natural and human influences are integrated through various quantitative factors, including climate variables (such as rainfall, wind speed, and snowfall), landform characteristics, soil roughness, vegetation cover, and tillage practices. Many of these factors are based on findings from previous studies, as detailed in the following methods section. Specifically, the P factor in the RUSLE model, which reflects soil loss reduction due to human management practices, is calculated as the ratio of soil loss observed in control experiment plots without protective measures to that observed in plots with conservation management, as described by Zhang et al. [21]. To simulate the spatial variation of the P factor under CT and NT practices in Northeast China, a dataset was compiled using annual soil loss amounts obtained from field observations documented in the peer-reviewed literature for the present study. Additionally, a new soil freezing factor (F) was developed in the present study, defined as the absence of soil loss induced by wind and water erosion under frozen conditions. This factor is specifically tailored for Northeast China, characterized by extremely low soil and air temperatures throughout the winter months each year. The equation for the FE factor is shown below. Finally, the spatial and temporal variability of soil erosion under CT and NT from 2010 to 2018 was projected onto a cropland map of Northeast China, and then the underlying mechanisms driving these erosions were analyzed in this study.

2. Materials and Methods

2.1. Study Area

The study investigates the black soil region of Northeast China (115°31′–135°05′ E, 38°43′–53°33′ N), covering an expansive land area of 1.25×10^6 km^2, comprising Heilongjiang, Jilin, and Liaoning provinces and the eastern segment of Inner Mongolia (Figure 1). Subsequently, this area is subdivided into five sub-regions based on distinct climatic and ecological characteristics: the Greater Kinggan Mountain, the Songnen Plain, the Liao River Plain, the Changbai Mountains, and the Sanjiang Plain regions, as depicted in Figure 1. Specifically, only arable lands that adopt conventional or conservation tillage practices and cultivate major crops such as soybean, maize, and wheat are estimated in the preset study, while paddy soils are excluded due to their lower soil erosion. Furthermore, the distribution of dryland in Northeast China is predominantly concentrated in the Songnen Plain, followed by the Greater Khingan Mountains regions, with statistical areas of 114.55×10^3 km^2 and 79.26×10^3 km^2, respectively, in 2018. The Changbai Mountains contain approximately 48.61×10^3 km^2 of dry land, ranking third in terms of area. Ultimately, the dryland areas in the Liao River Plain and Sanjiang Plain are comparatively lower, with statistical areas of 37.87×10^3 km^2 and 32.96×10^3 km^2, respectively (Figure 1).

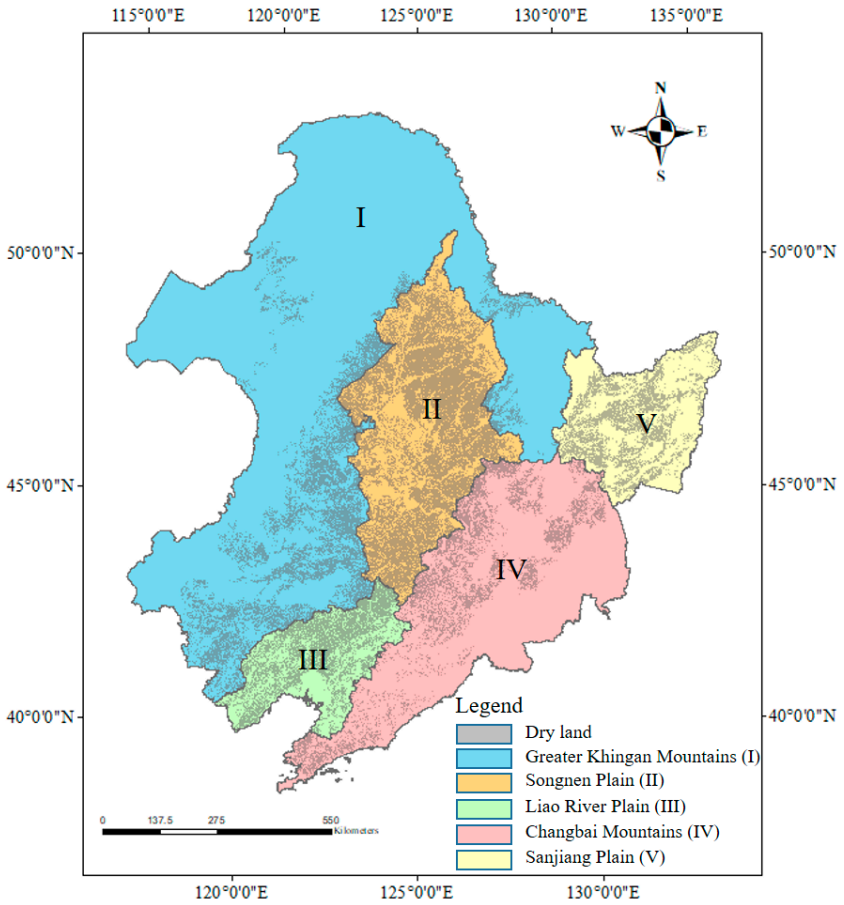

Figure 1. The distribution of dryland and the five ecological regions (I–V) in Northeast China.

2.2. Data Resource and Processing

Data on the daily rainfall, air temperature, wind speed, and snow cover of China mainland were downloaded from the China Meteorological Data Service Center (http://data.cma.cn/ accessed on 14 April 2024). Data on the soil sand, clay, silt, organic carbon contents, and cropland data of the Northeast China were obtained from the Resource and Environment Science and Data center (https:/www. resdc.cn/Default.aspx, accessed on 14 April 2024). Soil slope and surface 30 m resolution digital elevation mode (DEM) data were downloaded from the Geospatial Data Cloud (https://www. gsclod accessed on 14 April 2024). The monthly normalized difference vegetation index (NDVI) products came from the National Science Data Center (http://www.csdata.org/ accessed on 14 April 2024). Moreover, a local erosion dataset of different tillage practices was created by extracting the soil loss amount from water and wind erosion under CT and NT practices from 58 peer-reviewed literature [12–15,23–76] sources in the Northeast China. These papers were collected from various sources including Web of Science, Google Scholar, Springer Link, Scopus, and China Knowledge Resource Integrated Database (CNKI) during the period of 2010 to 2018. Subsequently, all the datasets were normalized to a standard resolution of 1 km^2 using the "GeoPandas" package within the Python software (version 3.7) for further analysis.

2.3. RUSLE Model

The water-induced soil erosion amount (E, expressed in Mg ha^{-1} yr^{-1}) under conventional tillage (CT) and conservation tillage (NT), separately, are estimated using the Revised Universal Soil Loss Equation (RUSLE; Equation (1)) by multiplying seven factors ad follows [77]:

$$E = R \cdot K \cdot L \cdot S \cdot C \cdot F \cdot P \quad (1)$$

Here, R is calculated as follows [24]:

$$Ri = a\sum_{1}^{n} Dj^{b} \tag{2}$$

Ri represents the rainfall-runoff erosivity force during the half month of i, measured in (MJ mm)/(ha^{-1} h^{-1}); Dj denotes the daily rainfall (mm) on day j within a specific half month period, with days receiving over 12 mm of rainfall noted, and otherwise the value is noted as 0; n represents the count of days with rainfall exceeding 12 mm in each half-month period; parameters a and b are directly derived from Zhang et al. [78], who computed these values for all of mainland China using nonlinear regression analysis, minimizing the sum of squared residuals using the Levenberg–Marquardt method. The 15th day of each month is chosen to divide one month into two half-months, resulting in 24 half-months per year.

$$\begin{array}{c} K = \left(0.2 + 0.3\exp\left(-0.0256Sa\left(1 - \frac{Si}{100}\right)\right)\right)\cdot\left(\frac{Si}{Ci-Si}\right)^{0.5}\cdot \\ \left(1 - \frac{0.25SOC}{SOC+\exp(3.72-2.95SOC)}\right)\cdot\left(1 - \frac{0.75Si}{Si+\exp(-5.51+22.95Si)}\right) \end{array} \tag{3}$$

The K factor represents the soil erodibility factor for water erosion; the Sa, Si, and Ci denote the soil sand, silt, and clay content, respectively, expressed as percentages. SOC indicates the soil organic carbon content, which is also expressed as a percentage.

$$L = (l/22.13)^{\alpha} \tag{4}$$

$$\alpha = \beta/(\beta + 1) \tag{5}$$

$$\beta = (sin\theta/0.0896)/\left[3.0(sin\theta)^{0.8} + 0.56\right] \tag{6}$$

$$S = \begin{cases} 10.8\ sin\theta + 0.03 & \theta < 9\% \\ 16.8\ sin\theta - 0.50 & 9\% < \theta < 14\% \\ 21.9\ sin\theta - 0.96 & \theta > 14\% \end{cases} \tag{7}$$

L and S factor denote the slope length and steepness factors, respectively, with l representing the slope length measured in meters and calculated from DEM using the following equation: DEM/ sin(θ*π/180). α and β represent the model parameters for slope length and steepness, while θ signifies the slope angle or gradient, expressed as a percentage.

$$C = \exp\left[-\alpha\cdot\frac{NDVI}{\beta - NDVI}\right] \tag{8}$$

The C factor indicates the effect of crop covering on soil water erosion, represented by a dimensionless value ranging from 0 to 1. The values of α and β, set at 2 and 1, respectively, are derived from Li et al. [79]. The Normalized Difference Vegetation Index (NDVI) represents the fractional vegetation cover calculated from remote sensing data acquired by MODIS.

$$F = \begin{cases} 1 & P(T > 0°C) \\ 0 & P(T < 0°C) \end{cases} \tag{9}$$

The soil freezing factor (F) has been introduced in the present study to account for the water-induced soil erosion halted by soil water freezing in the black soil region of Northeast China, particularly during winter rainy periods. The variable $P(T < 0)$ takes on the values of 0 or 1, indicating whether the air temperature is above or below 0 degrees Celsius, resulting in a corresponding value of 0 or 1 for F. A value of 0 for F signifies no soil erosion, while a value of 1 indicates the absence of freezing effects.

$$P = \frac{A_{NT}}{A_{CT}} \tag{10}$$

The P factor signifies the protective effect of conservation tillage practices against soil water erosion in the field. Here, A_{NT} represents the soil erosion amount in *NT* practices, while A_{CT} represents the soil erosion amount in *CT* practices.

2.4. RWEQ Model

Soil wind erosion under *CT* and *NT* systems was computed utilizing the Revised Wind Erosion Equation (RWEQ) model [80], which integrates empirical and process-based components, considering seven influencing factors. The model's formulas are provided below:

$$\mathrm{E}' = \frac{2z}{Qs^2} Q_{max}\, e^{-(\frac{z}{Qs})^2} \tag{11}$$

$$\mathrm{QS} = 150.71\left(WF{\cdot}K'{\cdot}SCF{\cdot}RN{\cdot}F'{\cdot}C'{\cdot}P'\right)^{-0.3711} \tag{12}$$

$$Q_{max} = 109\left(WF{\cdot}K'{\cdot}SCF{\cdot}RN{\cdot}F'{\cdot}C'{\cdot}P'\right) \tag{13}$$

where E′ represents the wind-induced soil loss amount (E′, measured in units of t ha^{-1} a^{-1}); QS denotes the critical field length for determining wind erodibility in specific areas, with a unit of meters (m); Q_{max} signifies the maximum transport capacity of soil sediment by wind erosion in a field (kg m^{-1}); and Z represents the downwind maximum distance at which the maximum wind erosion occurs, with a fixed value of 50 m in the present study.

$$\mathrm{WF} = W_f{\cdot}\frac{\rho}{g}{\cdot}SW{\cdot}SD \tag{14}$$

$$W_f = \frac{\sum_1^n v_2(v_2 - v_1)^2}{n} \cdot n_d \tag{15}$$

$$\mathrm{SW} = \frac{ET_p - (R + I){\cdot}\frac{R_d}{N_d}}{ET_p} \tag{16}$$

$$\mathrm{SD} = 1 - \mathrm{P}(H_{snow} > 25.4\mathrm{mm}) \tag{17}$$

WF is the weather factor component computed from the wind forces (W_f), soil wetness index (SW), and the snow cover depth (SD). Here, ρ and g represent the air density and the gravitational acceleration, respectively, with fixed values of 1.29 kg m^{-3} and 9.81 m s^{-2}, respectively; n is the number of wind-erosion events in each month; N_d is the total number of these events; v_1 is the threshold wind speed set at the standard of 5 m s^{-1} in this study; and v_2 represents the observed wind speed at a height of 10 m (m s^{-1}). ET_p represents the potential evapotranspiration, while R and I represent the daily rainfall amount (mm) and irrigation (mm), with Rd and Nd denoting the number and total number of rainfall and/or irrigation days within each month, respectively. In this study, the I was set to 0 mm given that Northeast China is a region reliant on rainfall, without the presence of irrigation practices. Furthermore, P(H_{snow} > 25.4 mm) represents the probability of the snow depth exceeding 25.4 mm.

$$\mathrm{K}' = \frac{29.09 + 0.31Sa + 0.17Si + 0.33\left(\frac{Sa}{Ci}\right) - 2.59SOM - 0.95CaCO_3}{100} \tag{18}$$

$$\mathrm{SCF} = \frac{1}{1 + 0.0066Ci^2 + 0.021SOM^2} \tag{19}$$

K′ and SCF represent the soil erodibility factor for wind erosion and the soil crust factor, respectively, where *Sa*, *Si*, and *Ci* denote the soil sand, silt, and clay content, respectively, as mentioned previously. *SOM* is calculated from *SOC*, while $CaCO_3$ is not considered here.

$$\mathrm{RN} = e^{(1.86RN_r - 2.41RN_r^{0.94} - 0.127C_{rr})} \tag{20}$$

$$RN_r = 0.2\,\frac{RH^2}{RS} \tag{21}$$

$$C_{rr} = 17.46\,RR^{0.738} \tag{22}$$

Here, RN represents the soil roughness factor (dimensionless), with *RNr* indicating ridge or oriented roughness, *Crr* representing chain random roughness, and *RR* denoting aggregate roughness. *RH* and *RS* represent ridge height (cm) and ridge spacing (cm), respectively, as derived from the DEM in Northeast China.

Furthermore, the F′ and P′ factors for wind erosion as affected by soil freezing and conservation tillage protection are calculated following similar formulations as the water erosion equations as mentioned previously in Equations (9) and (10).

$$C' = e^{-0.043 \cdot SC} \tag{23}$$

$$\mathrm{SC} = \frac{NDVI - NDVI_{min}}{NDVI_{max} - NDVI_{min}} \tag{24}$$

Similarly, the C′ factor denotes the influence of crop covering on wind erosion, using the *NDVI* data mentioned previously in Equation (8).

2.5. Subsection

The Soil Erosion Classification Standard (SL190–2007) from the People's Republic of China was employed to categorize the simulated water and wind erosion into several levels for evaluating the black soil erosion risks under CT and NT practices. These classifications include tolerable, slight, moderate, severe, very severe, and destructive erosion, defined by thresholds of 0–200, 200–2500, 2500–5000, 5000–8000, 8000–15,000, and (>15,000) t km^{-2} a^{-1}, respectively.

2.6. Model Accuracy

To assess the accuracy of the RUSLE and RWEQ models in this study, linear regression was performed between the simulation results and the measurement data obtained from the publications included in the tillage dataset as mentioned above. Additionally, the root mean square error (RMSE), mean absolute error (MAE), and R-square between the simulation and measurement were calculated using the equations from Wang et al. [81].

3. Results

3.1. Model Factors

The results derived from the RUSLE and RWEQ models are illustrated in Figures 2 and 3. The R factor demonstrated a significant range from 167.2 to 7896.4 MJ mm hm^{-2} h^{-1} a^{-1} across the entirety of the black soil region, particularly pronounced in the southern parts of Northeast China (Figure 2A). The K factor was low in the Songnen plain but high in the Liao River plain, corresponding well to the spatial pattern of soil clay content [82]. Furthermore, soil L and S factors are generally greater in mountainous than flat plain regions. The C factor notably decreased from 1 to 0.1 during May to June within arable land during the growth of crops and then stabilized until October when crop harvest (Figures 2c and S1). The F factor remained at 0 throughout the entire winter and transitioned to 1 as soil ice melted in March each year (Figure S2). Ultimately, the P factor of NT increased from 0.10 to 0.21 spatially, but temporal evaluation was hindered by data scarcity (Figure 2F). For comparison, the P factor of CT was set to 1 in the RUSLE model.

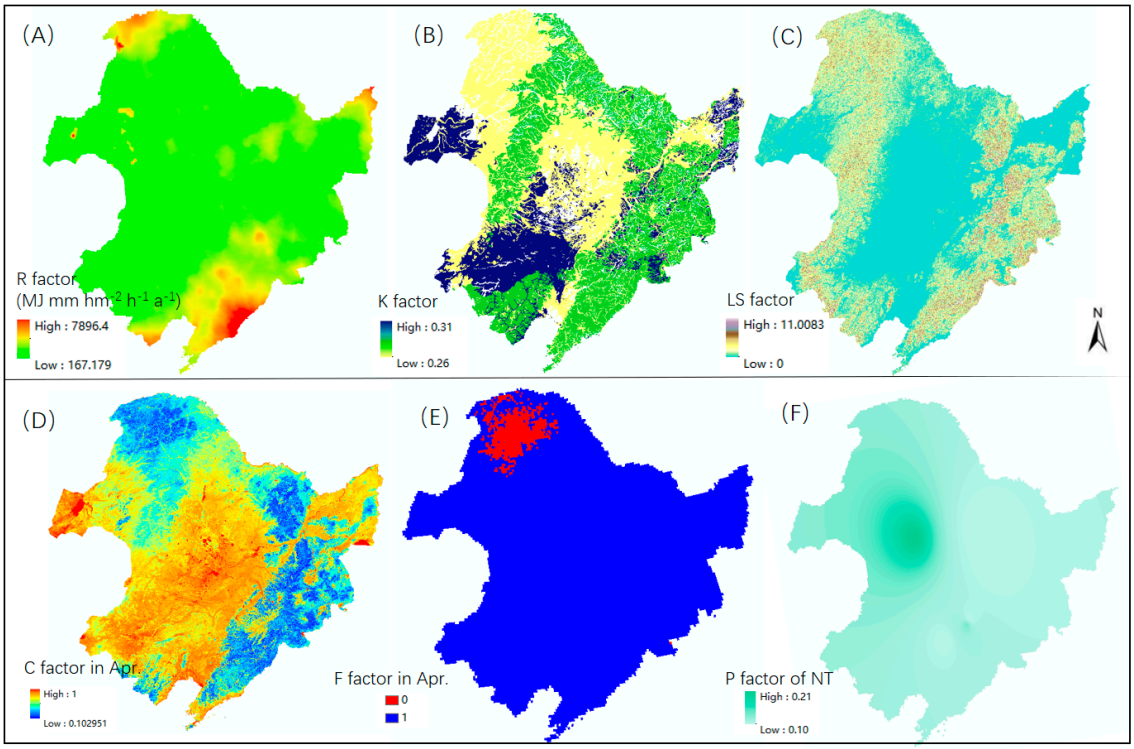

Figure 2. Spatial distribution of factors in the RUSLE model under different tillage practices in 2018, including rainfall erosivity, R (**A**); soil erodibility, K (**B**); slope length and steepness, LS (**C**); crop covering, C (**D**); soil frozen factor, F (**E**); and protected effect of conservation tillage, P (**F**).

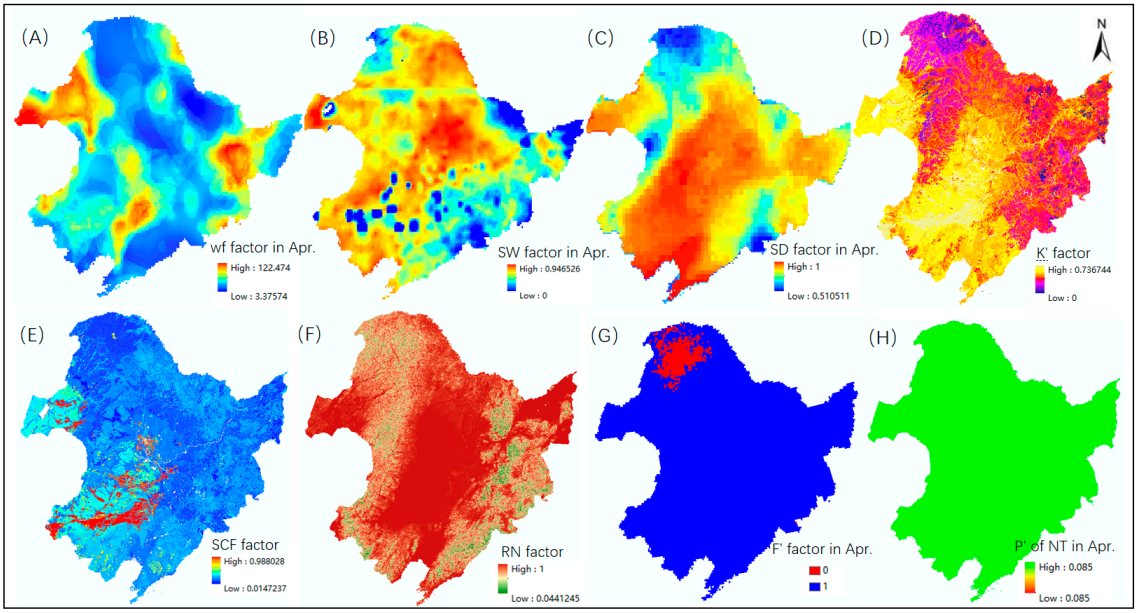

Figure 3. Spatial distribution of factors in the RWEQ model under different tillage practices in 2018, including wind erosivity, W_f (**A**); soil wetness, SW (**B**); snow cover depth, SD (**C**); soil erodibility factor, K′ (**D**); soil curst factor, SCF (**E**); soil roughness, RN (**F**); soil frozen factor, F′ (**G**); and straw protection of conservation tillage, P′ (**H**).

In the black soil region, the distribution of wind forces (W_f) in the RWEQ model were highly scattered (Figure 3A). Moreover, soil SW, surface SD, and F′ factors varied across different areas, weather conditions, and/or seasons (Figures 3B,C,G, and S1). Soil K′ factors were higher in the north and east, while the SCF factor was greater in the west and south

areas, with soil RN factor being higher in the central regions (Figure 3D–F). Similarly, the P′ factor for wind erosion was set as 1 for CT and varied from 0.99 to 0.085 due to increased straw covering and reduced soil disturbance in NT over the months (Figures 3H and S4).

3.2. Spatial Patterns of Soil Erosion as Affected by NT Practice

Soil water and wind erosion were widely distributed in the arable land of Northeast China (Figure 4). The regional average estimated 2603 t km^{-2} a^{-1} of water erosion and 34 t km^{-2} a^{-1} of wind erosion across the entire black soil region under CT practices in 2018 (Figure 4A,D; Table 1). These values were reduced by 56.4% and 91.8% with NT practices, respectively (Figure 4B,E; Table 1). Consequently, this reduction was more pronounced in the Changbai Mountains for water erosion and in the southwest of the Greater Khingan Mountains for wind erosion, where the intensity of water and wind erosion was most evidently observed corresponding (Figure 4C,F; Table 1). In the Changbai Mountain, soil areas of water erosion classified as very severe (8.03×10^3 km^2) and severe (7.62×10^3 km^2) under CT practices thereby reduced to only 2.31×10^3 km^2 and 5.61×10^3 km^2 under NT practices, respectively (Figure 5A). Meanwhile, the areas of wind erosion in the Greater Khingan Mountains shifted from 1.59×10^3 km^2 (class moderate) and 4.31×10^3 km^2 (class slight) under CT to 0 km^2 under NT (Figure 5B).

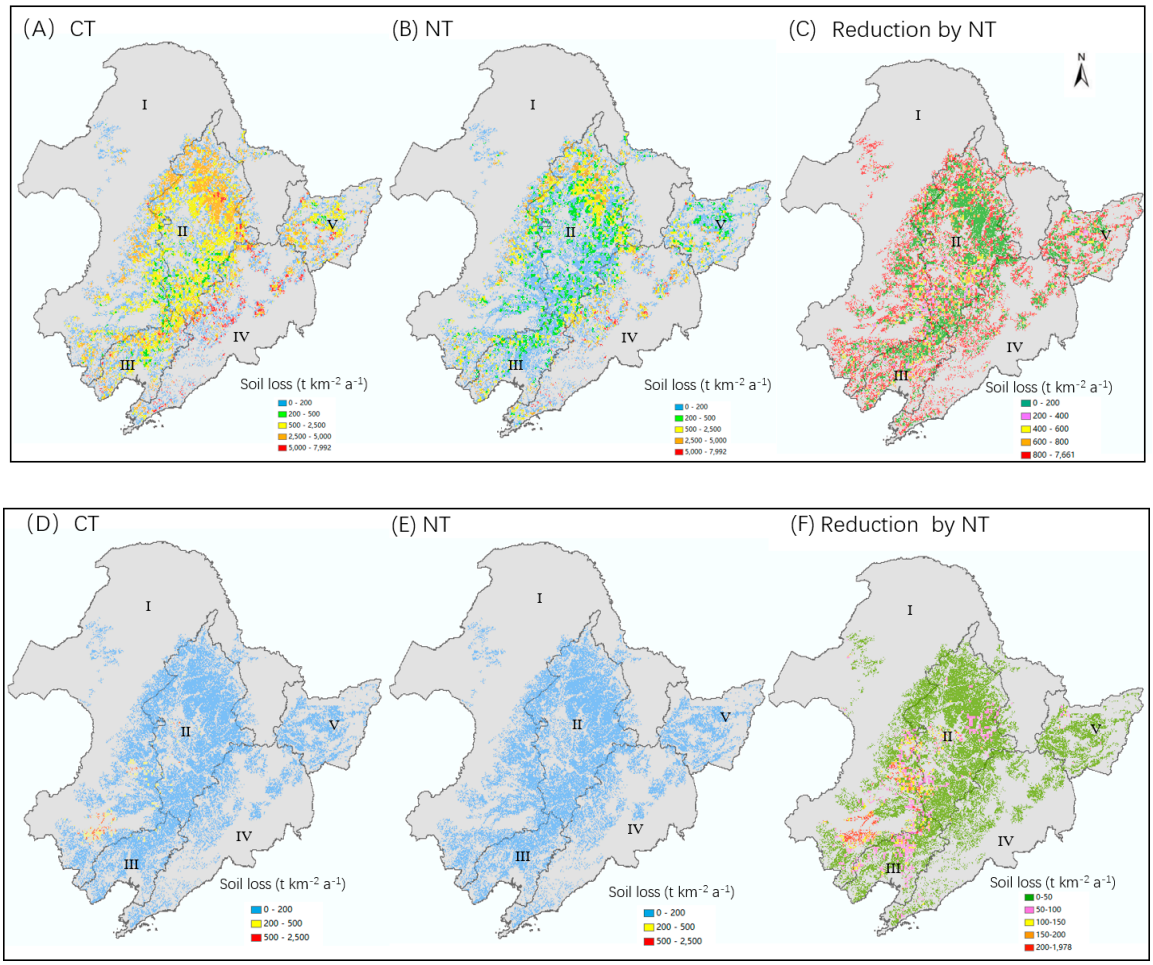

Figure 4. Spatial distribution of the water (**A**–**C**) and wind (**D**–**F**) erosion under different tillage practices in Northeast China's dryland in 2018. The five ecological regions are the Greater Khingan Mountains (I), the Songnen Plain (II), the Liao River Plain (III), the Changbai Mountains (IV), and the Sanjiang Plain (V).

Table 1. Average soil loss of different conservation regions under CT and NT practices in the black soil regions in Northeast China.

Regions	Water Erosion (t km^{-2} a^{-1})			Wind Erosion (t km^{-2} a^{-1})		
	CT	NT	Reduction	CT	NT	Reduction
I	2196	999	1206	70	6	64
II	2279	829	1457	24	2	22
III	2327	821	1508	40	3	37
IV	4370	2470	1895	7	1	6
V	2454	959	1489	13	1	12
Total	2603	1134	1511	34	2.8	28.2

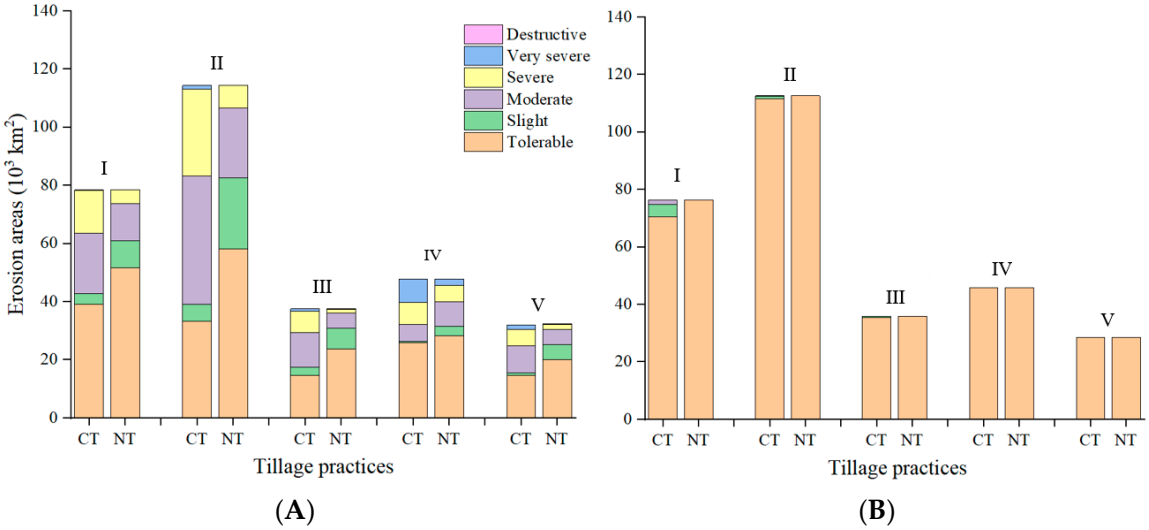

Figure 5. Areas of water (**A**) and wind (**B**) erosion under different tillage practices exhibited several grades in Northeast China in 2018. The six erosion grades include tolerable (0–200 t km^{-2} a^{-1}), slight (200–2500 t km^{-2} a^{-1}), moderate (2500–5000 t km^{-2} a^{-1}), severe (5000–8000 t km^{-2} a^{-1}), very severe (8000–15, 000 t km^{-2} a^{-1}), and destructive erosion (>15, 000 t km^{-2} a^{-1}). The five ecological regions are the Greater Khingan Mountains (I), the Songnen Plain (II), the Liao River Plain (III), the Changbai Mountains (IV), and the Sanjiang Plain (V).

Considering area, the largest water and wind erosion areas were observed in the Songnen plain, which encompasses the majority of arable land in Northeast China (Figures 4 and 5). Here, soil erosion caused by water was significantly higher than that caused by wind, with the highest water-induced erosion areas predominantly distributed in the northeast part of the plain (Figure 4). Similarly, NT practice significantly reduced high-level erosion. Under NT, areas previously subjected to soil water erosion classified as moderate, severe, and very severe under CT decreased to tolerable and slight levels, with the areas of very severe reduced to 0 km^2 (Figure 5A). The average change in soil amount caused by water erosion therefore declined from 2327 t km^{-2} a^{-1} in CT to only 821 t km^{-2} a^{-1} under NT in this plain (Table 1).

In the Liao River and Sanjiang plains, both the intensity and areas of water erosion were estimated to be low, and there was no obvious wind erosion observed (Figures 4 and 5; Table 1). However, the potential reduction of water erosion caused by NT practice was still significant in specific areas within these regions (Figure 4C). Furthermore, detailed soil erosion amounts and areas under CT and NT across the other arable land of Northeast China are presented in Figure 5 and Table 1.

3.3. Temporal Dynamics of Soil Erosion as Affected by NT Practice

The average annual and monthly soil loss amount was computed from 2010 to 2018 in this study (Figures 6 and 7). The annual average of soil loss amount due to water erosion remained relatively stable over these nine years, while the values for wind erosion fluctuated sharply, decreasing, increasing, and then decreasing again under CT treatments (Figure 6). Consequently, the monthly average soil loss amount due to water erosion under CT and NT was near zero t km^{-2} m^{-1} at the beginning (January, February, March) and the end (November, December) of each year in Northeast China (Figure 7A). It initially increased from 39.4 ± 21.2 t km^{-2} m^{-1} to 165.7 ± 44.0 t km^{-2} m^{-1} from April to July and then steadily decreased to 0 by November under CT practices. From April to October, soil water erosion was proportionally reduced by NT compared to CT. The greatest reduction was observed from June to August, with lower reductions in May, September, and October. For wind erosion, soil loss was observed annually under CT from March to May, with a predominance in the latter two months. Furthermore, this wind erosion was reduced by 91.5% under NT practices in each month (Figure 7B).

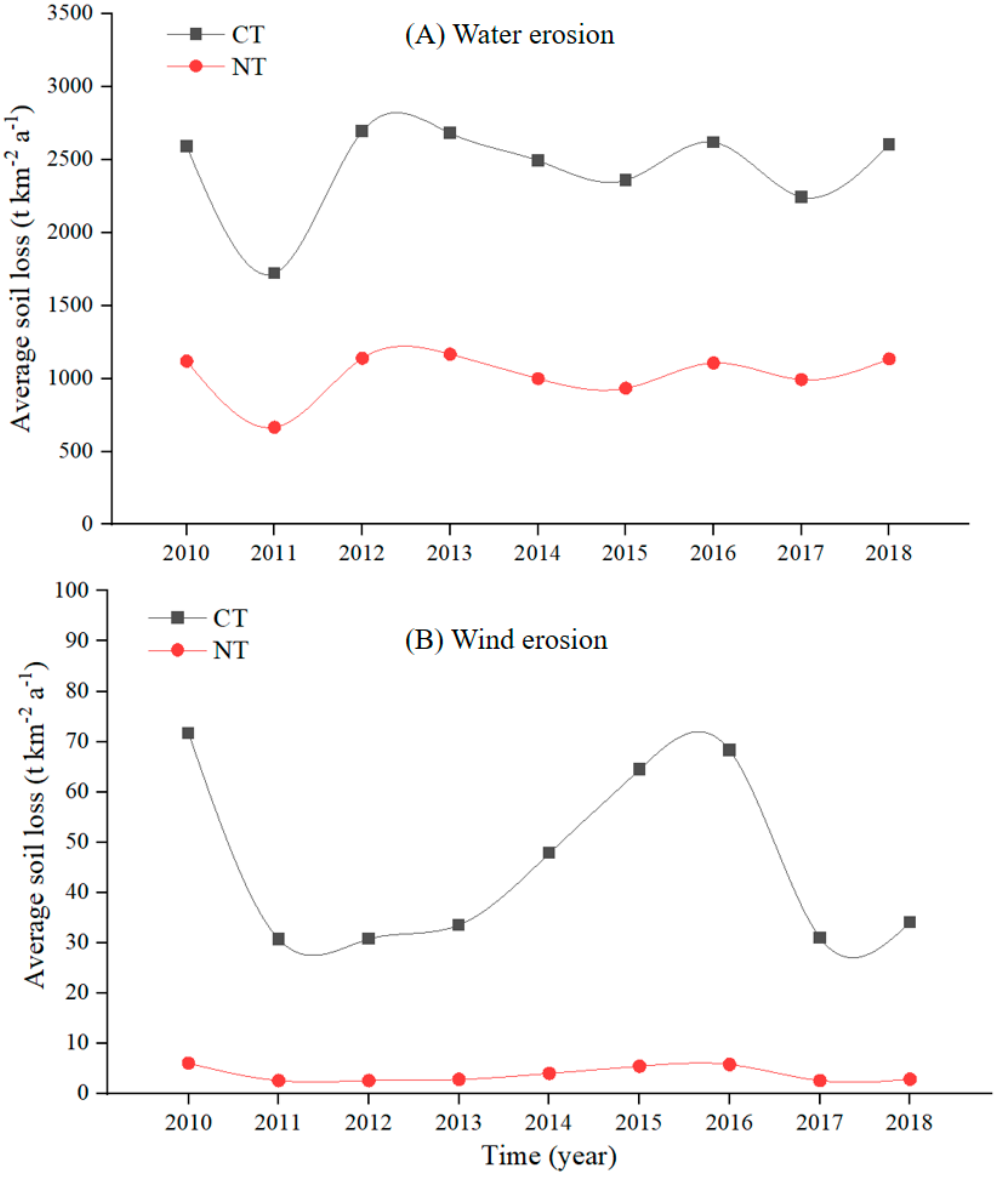

Figure 6. Annually change in soil loss via water (**A**) and wind (**B**) erosion under different tillage practices in Northeast China's dryland.

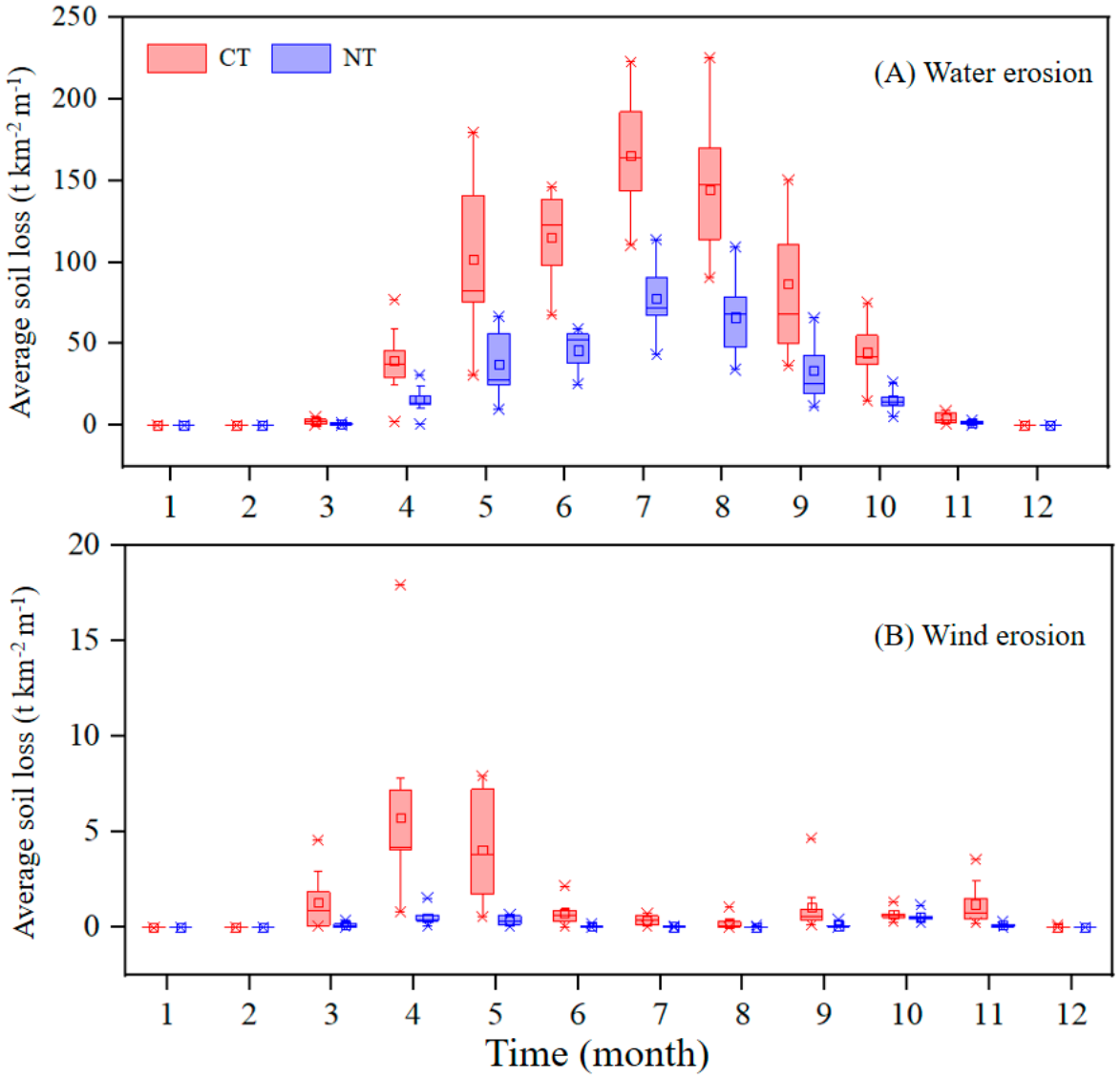

Figure 7. Monthly change in soil loss via water (**A**) and wind (**B**) erosion under different tillage practices in Northeast China's dryland.

3.4. Influence of Various Factors on Soil Erosion as Affected by NT Practice

In Northeast China, water erosion was mainly influenced by precipitation, while wind erosion was driven by wind speed (Figure 8). Under CT and NT practices, precipitation contributed 24.9% and 30.9% to soil water erosion, respectively, while wind speed contributed 26.5% and 26.9% to soil wind erosion, respectively. Consequently, field slope, soil clay content, and local aridity index significantly influenced soil loss under water erosion in both CT and NT practices (Figure 8A). Wind erosion, on the other hand, was notably influenced by arid conditions, soil silt content, field length, and local precipitation under both tillage practices in the same regions (Figure 8B).

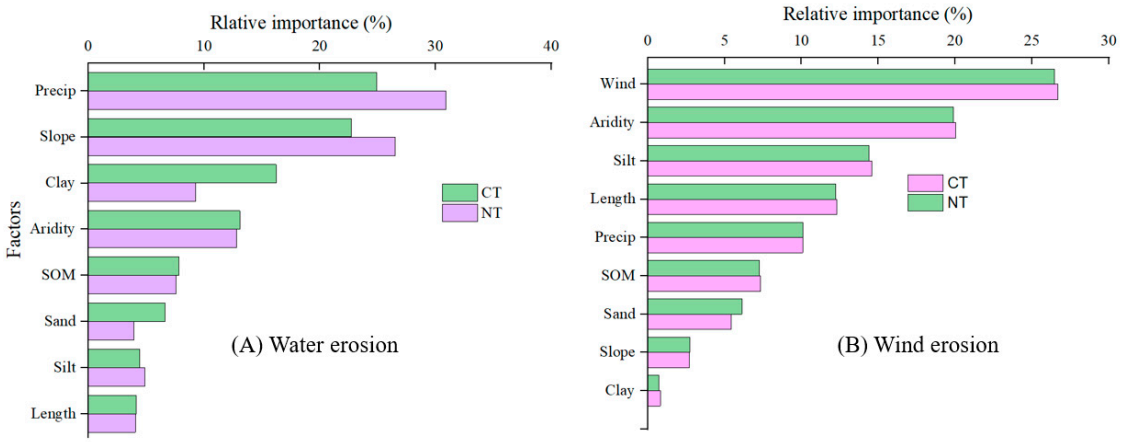

Figure 8. The effect of various factors on soil water (**A**) and wind (**B**) erosion under different tillage practices in Northeast China's dryland in 2018.

4. Discussion

4.1. Model Validation

Our models performed well in simulating the variation of soil wind and water erosion under CT and NT practices in the dry lands of Northeast China, with credible model evaluation indices of R^2 (0.65, 0.56, and 0.66), MAE (891, 409, and 151), and RMSE (1277, 916, and 268) for the RUSLE-CT, RUSLE-NT, and RWEQ-NT models, respectively (Table 2). However, the correlation between simulated and measured soil loss under wind erosion in the RWEQ-CT model is poor (R^2: 0.15, MAE: 262, RMSE: 425; Table 2), primarily due to the limited number of verification data and their concentrated distribution, with only five observations mainly in eastern Inner Mongolia.

Table 2. Performance of the RUSLE and RWEQ models as evaluated by the correlation between the simulated and measured data (collected from the publications).

Erosion	Tillage	Number	The Relationship between the Simulated and Observed Data	MAE	RMSE	R^2
Water	CT	44	y = 0.2377× −3.6909	891	1277	0.65
	NT	39	y = 0.0772× +53.263	409	916	0.56
Wind	CT	5	y = 1.1519× +110.45	262	425	0.15
	NT	9	y = 0.7060× −10.943	151	268	0.66

Furthermore, our simulated water erosion values under CT across the cropland of Northeast China, at light and higher levels, covered an area of 182,265.52 km^2 in 2015. This value closely aligns with the 181,130.18 km^2 reported in the National Soil Erosion Investigation of China (NSEI-C) conducted by the Chinese Academy of Sciences (CAS) in 2015, using an integrated evaluation method [83]. However, our estimation of wind erosion under CT for the same year and levels amounted to only 74,223.85 km^2, which is significantly lower than the 99,210.43 km^2 reported by the NSEI-C. This disparity may be attributed to the fact that our research focused solely on cropland, while their study included a broader range of land uses. Moreover, the spatial patterns of wind and water erosion distribution under CT practice closely resembled those observed in several previous studies [7,83,84]. We failed to compare the NT results with those of other models due to the lack of corresponding predictions in the current regions.

4.2. Spatial Patterns of Soil Erosion as Affected by NT Practice

NT practices in the mountainous regions (Changbai Mountains, Greater Khingan Mountains) demonstrated the highest efficiency in conserving soil water and wind erosion

(Figure 4). This can be primarily attributed to the fact that these areas are among the most severely eroded regions in Northeast China. Furthermore, precipitation and cropland slope contributed the most at approximately 30.9% and 26.5%, respectively, to soil water erosion under NT practices on the spatial scale (Figure 7). Precipitation primarily drove soil runoff in croplands [78]. However, in the Changbai Mountains regions, the R factor of the rainfall and runoff erosivity force was not the highest (Figure 2A), indicating that the steeper slopes of croplands in these areas were the main reason for more severe soil water erosion (Figure 2C). The intensity of water erosion significantly increased with soil slopes from 5° to 18° under CT in the mountainous regions (Figure 9), attributed to increased runoff with steeper slopes during rainfall events [85]. Additionally, the loosened soil structure, breakdown of soil aggregates, and removal of residue coverage by mechanical till disturbance exacerbated soil loss induced by water runoff in the mountains areas [60]. In contrast, under NT practices, soil mulched by straw residue and soil structure stability improved due to continuous non-disturbance from no-tillage practices [86]. Consequently, surface sealing formation declined and water infiltration increased, resulting in a significant reduction of surface runoff and providing a mechanical barrier to soil displacement [87]. Subsequently, this cover under NT also reduced wind-induced soil erosion in the Greater Khingan Mountains regions, where the most severe wind erosion occurred due to high wind speeds and dry climate conditions [88]. Notably, the success of NT in soil erosion conservation in mountainous regions does not imply its failure in plain regions, where the substantial reduction gap observed in erosion reduction was due to the highest initial erosion values occurring under CT practices.

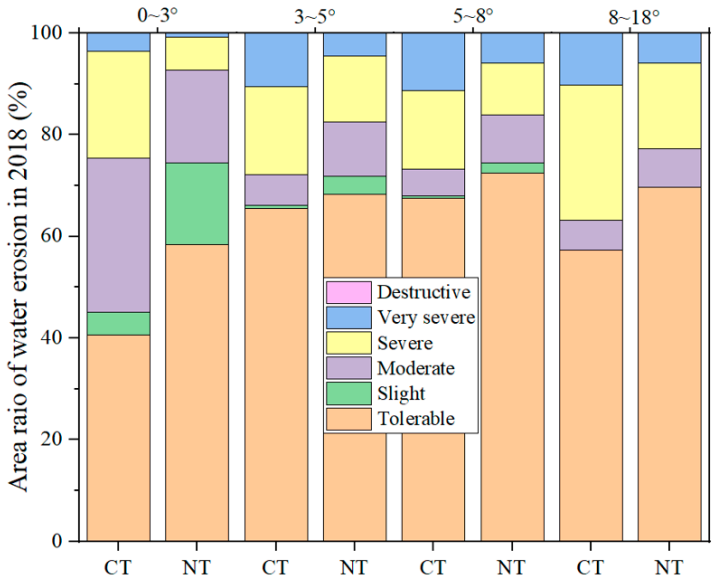

Figure 9. Relationship between soil water erosion and slope under different tillage practices in Northeast China's dryland in 2018. The slope of the arable land ranged 0–18° in the areas, with 0–5° representing plain areas and 5–18° representing mountainous regions.

In the plain areas such as the Songnen, Liao River, and Sanjiang plains, the regions experiencing wind erosion at light and higher levels (defined as noticeable soil loss) were estimated to be near zero under both CT and NT practices, owing to the absence of strong wind events in these areas (Figure 5). This finding is consistent with Wang et al. [81]. Furthermore, water erosion at light and higher levels was widespread and significantly reduced by NT compared to CT practices (Figure 4), particularly in the Songnen plain, which has the largest area of arable lands in Northeast China. Furthermore, severe (light and higher) water erosion was observed more frequently in small arable land slopes of 0~3° than in higher slope areas of 3~5° in the plain regions (Figure 9), consistent with the

findings of Wang et al. [30]. This suggests a pronounced pattern of precipitation driving soil loss under the topographical features of long gentle slopes [85].

4.3. Temporal Dynamics of Soil Erosion as Affected by NT Practice

Annually, soil water and wind erosion under CT and NT fluctuated with local climate variations (rainfall and wind speed, Figure 6), as well-documented [60,84,89]. Interestingly, on a monthly basis, soil wind and water erosion cease in January, February, November, and December each year in the arable land of Northeast China (Figure 7). This cessation is attributed to the snow covering and soil water freezing under the extremely cold climate in this area. The seasonal average surface air temperature was lower than −15 °C during the winter from 2010 to 2018 in this study (data not shown), resulting in soil freezing to depths of over 200 cm per year, as observed by Xu et al. [90] in Heilongjiang province. This result highlights the significant benefit of naturally lower temperatures in reducing black soil loss through erosion during the long winter period each year.

Consequently, this frozen state of the soil water continues until early March each year (Figure S2), and then the ice begins to melt from the south to the north of Northeast China within this month (Figure 6). Thus, slight wind erosion occurs in March, particularly in the early warmer areas of southern Northeast, but there is no water erosion due to lack of rainfall during this period [91]. Furthermore, black soil experiences concentrated wind erosion in April and May each year under CT practices, primarily due to high levels of soil disturbance and the removal of residue cover. Conversely, these highest wind erosion rates were significantly reduced to near zero by NT, owing to mulching and the preservation of undisturbed soil structure [14]. This finding suggests that the greatest benefits of conservation tillage on mitigate soil loss by wind erosion occur in April and May, preceding the planting season each year. This provides valuable information for directing focus toward wind erosion conservation efforts during these two months.

Subsequently, soil water erosion under CT sharply increases from May to June, peaking in July, which aligns with the maize growth season. From August to September, black soil loss due to water erosion diminishes. This reduction is attributed to the dense canopy of maize, which mitigates the direct impact of raindrops on the soil surface [92] and extends the time taken for water to reach the soil, thereby reducing surface runoff [87,93]. During the entire process, soil water erosion was proportionally reduced by NT practices (Figure 6). However, we were unable to provide detailed insights into the performance of NT on water erosion within monthly dimensions due to the lack of supervisory data. This underscores the necessity for further measurements and research in the future.

4.4. The Implementation of NT Practice in Northeast China

Overall, NT practice shows enormous potential in reducing soil erosion and preserving the ecological benefits of black soil. However, the current adoption of conservation tillage in black soil regions of China remains limited [79,94], possibly due to the yield decrease associated with NT [95]. Therefore, striking a balance between economic gains and ecological benefits in this region will be a worthwhile issue to address. Based on the results of this study, specific recommendations for NT practices are as follows: (i) NT with straw mulching is most suitable in the southern regions of the Greater Khingan Mountains and Songnen Plain, the entire Liao River Plain, and the Changbai Mountains, where it demonstrates the highest efficiency for conserving soil erosion (water and wind), and it has been shown to achieve higher yields according to our previous study [96]. (ii) Caution is needed when implementing NT in the northern regions of the Songnen Plain and the Sanjiang Plain. In these areas, the reduction of soil erosion was minimal (Figure 4), and yields of NT were reduced [96]. (iii) Continuous monitoring of soil erosion and crop yields under NT practices is essential. The data collected should be used to refine and adapt NT techniques to local conditions, ensuring that both ecological and economic benefits are maximized.

5. Conclusions

In Northeast China's arable lands, conventional tillage (CT) leads to intense and widespread soil water and wind erosion. No tillage (NT) with straw mulching significantly reduces these erosive processes. Soil erosion ceases in winter under both systems, with NT showing a marked reduction in soil loss from spring to autumn compared to CT. Spatial distribution maps revealed that NT is most effective in conserving soil in mountainous regions. Based on existing data, NT is best suitable in the southern regions of Northeast China for maintaining soil health and crop yields, while its effectiveness diminishes in the northern and eastern regions.

Supplementary Materials: The following supporting information can be downloaded at: https://www.mdpi.com/article/10.3390/land13081219/s1.

Author Contributions: Investigation, F.J. and Y.Q.; writing—original draft preparation, F.J.; writing—review and editing, X.P. and Z.Z.; project administration, Q.L.; funding acquisition, Q.L. All authors have read and agreed to the published version of the manuscript.

Funding: This research was funded by the National Natural Science Foundation of China, grant number U23A20222; and by the National Key Research and Development Program of China, grant number 2022YFD1500905-04.

Data Availability Statement: Data will be available on request.

Conflicts of Interest: The authors declare that they have no known competing financial interests or personal relationships that could have appeared to influence the work reported in this paper.

References

1. Borrelli, P.; Robinson, D.A.; Fleischer, L.R.; Lugato, E.; Ballabio, C.; Alewell, C.; Meusburger, K.; Modugno, S.; Schutt, B.; Ferro, V.; et al. An assessment of the global impact of 21st century land use change on soil erosion. *Nat. Commun.* **2017**, *8*, 2013. [CrossRef] [PubMed]
2. Yang, G.; Sun, R.; Jing, Y.; Xiong, M.; Li, J.; Chen, L. Global assessment of wind erosion based on a spatially distributed RWEQ model. *Prog. Phys. Geogr.* **2021**, *46*, 28–42. [CrossRef]
3. Chi, W.; Zhao, Y.; Kuang, W.; He, H. Impacts of anthropogenic land use/cover changes on soil wind erosion in China. *Sci. Total Environ.* **2019**, *668*, 204–215. [CrossRef] [PubMed]
4. Lu, S.; Duan, X.; Wei, S.; Lin, H. An insight to calculate soil conservation service. *Geogr. Sustain.* **2022**, *3*, 237–245. [CrossRef]
5. Li, C.; Fu, B.; Wang, S.; Stringer, L.C.; Wang, Y.; Li, Z.; Liu, Y.; Zhou, W. Drivers and impacts of changes in China's drylands. *Nat. Rev. Earth Environ.* **2021**, *2*, 858–873. [CrossRef]
6. Li, Z.; Wang, S.; Li, C.; Ye, C.; Gao, D.; Chen, P. The trend shift caused by ecological restoration accelerates the vegetation greening of China's drylands since the 1980s. *Environ. Res. Lett.* **2022**, *17*, 044062. [CrossRef]
7. Wang, S.; Xu, X.; Huang, L. Spatial and Temporal Variability of Soil Erosion in Northeast China from 2000 to 2020. *Remote Sens.* **2022**, *15*, 225. [CrossRef]
8. Wang, H.; Yang, S.; Wang, Y.; Gu, Z.; Xiong, S.; Huang, X.; Sun, M.; Zhang, S.; Guo, L.; Cui, J.; et al. Rates and causes of black soil erosion in Northeast China. *Catena* **2022**, *214*, 106250. [CrossRef]
9. Chen, X.W.; Liang, A.Z.; Jia, S.X.; Zhang, X.P.; Wei, S.C. Impact of tillage on physical characteristics in a Mollisol of Northeast China. *Plant Soil Environ.* **2014**, *60*, 309–313. [CrossRef]
10. He, C.; Niu, J.R.; Xu, C.T.; Han, S.W.; Bai, W.; Song, Q.L.; Dang, Y.P.; Zhang, H.L. Effect of conservation tillage on crop yield and soil organic carbon in Northeast China: A meta-analysis. *Soil Use Manag.* **2022**, *38*, 1146–1161. [CrossRef]
11. Zhao, P.; Li, S.; Wang, E.; Chen, X.; Deng, J.; Zhao, Y. Tillage erosion and its effect on spatial variations of soil organic carbon in the black soil region of China. *Soil Tillage Res.* **2018**, *178*, 72–81. [CrossRef]
12. Zhang, S.; Zhang, X.; Huffman, T.; Liu, X.; Yang, J. Soil Loss, Crop Growth, and Economic Margins under Different Management Systems on a Sloping Field in the Black Soil Area of Northeast China. *J. Sustain. Agric.* **2011**, *35*, 293–311. [CrossRef]
13. Wang, J.; Shi, X.; Li, Z.; Zhang, Y.; Liu, Y.; Peng, Y. Responses of runoff and soil erosion to planting pattern, row direction, and straw mulching on sloped farmland in the corn belt of northeast China. *Agric. Water Manag.* **2021**, *253*, 106935. [CrossRef]
14. Jia, H.; Wang, G.; Guo, L.; Zhuang, J.; Tang, L. Wind erosion control utilizing standing corn residue in Northeast China. *Soil Tillage Res.* **2015**, *153*, 112–119. [CrossRef]
15. Chen, S.; Zhang, X.; Li, J.; Guo, M.; Hu, W. Effect of tillage management on the wind erosion of arable soil in the Chinese Mollisol region. *Front. Environ. Sci.* **2022**, *10*, 954004. [CrossRef]
16. Brooks, E.S.; Dobre, M.; Elliot, W.J.; Wu, J.Q.; Boll, J. Watershed-scale evaluation of the Water Erosion Prediction Project (WEPP) model in the Lake Tahoe basin. *J. Hydrol.* **2016**, *533*, 389–402. [CrossRef]

17. Flanagan, D.C.; Ascough, J.C.; Nearing, M.A.; Laflen, J.M. The Water Erosion Prediction Project (WEPP) Model. In *Landscape Erosion and Evolution Modeling*; Harmon, R.S., Doe, W.W., Eds.; Springer: Boston, MA, USA, 2001; pp. 145–199.
18. De Roo, A.P.J.; Offermans, R.J.E.; Cremers, N.H.D.T. LISEM: A single-event, physically based hydrological and soil erosion model for drainage basins. II: Sensitivity analysis, validation and application. *Hydrol. Process.* **1996**, *10*, 1119–1126. [CrossRef]
19. Morgan, R.P.C.; Quinton, J.N.; Smith, R.E.; Govers, G.; Poesen, J.W.A.; Auerswald, K.; Chisci, G.; Torri, D.; Styczen, M.E. The European Soil Erosion Model (EUROSEM): A dynamic approach for predicting sediment transport from fields and small catchments. *Earth Surf. Process. Landf.* **1998**, *23*, 527–544. [CrossRef]
20. Ghosal, K.; Das Bhattacharya, S. A Review of RUSLE Model. *J. Indian Soc. Remote Sens.* **2020**, *48*, 689–707. [CrossRef]
21. Zhang, X.K.; Xu, J.H.; Lu, X.Q.; Deng, Y.J.; Gao, D.W. A study on the soil loss equation in Heilongjiang province. *Bull. Soil Water Conserv.* **1992**, *12*, 1–10. (In Chinese with English abstract).
22. Jarrah, M.; Mayel, S.; Tatarko, J.; Funk, R.; Kuka, K. A review of wind erosion models: Data requirements, processes, and validity. *Catena* **2020**, *187*, 104388. [CrossRef]
23. Zhang, Q.H. The effect of different tillage and cover crop on the loss of soil nutrients. *Mod. Agri.* **2014**, *2*, 18–21. (In Chinese with English abstract).
24. Song, Y.; Zhang, Z.X. The effect of different tillage measures on soil erosion in slope farmland in black soil region. *Res. Soil Water Conserv.* **2011**, *18*, 14–16. (In Chinese with English abstract).
25. Chen, G.; Li, S.Q.; Li, J.W.; Fan, H.F.; Xie, Y. The initial analysis of sedemient reduction under soil and water conservation practices in the black soil region of Northeast China. *Soil Water Conser. Appl.* **2006**, *5*, 46–48. (In Chinese with English abstract).
26. Han, F.W.; Zhang, B.; Song, K.S.; Wang, Z.M.; Wang, Y.S.; Zhang, X.W. Study on the effect of soil erosion reduction corresponding to water and soil conservation measures in Heilongjiang low mountains area. *Sys. Sci. Compre. Stu. Agri.* **2007**, *23*, 407–410. (In Chinese with English abstract).
27. Qi, Z.J.; Zhang, Z.X.; Yang, A.Z. Benefit of soil and water conservation measures on sloping land of black soils. *Res. Soil Water Conser.* **2011**, *18*, 72–75. (In Chinese with English abstract).
28. Zhao, Y.S.; Wei, Y.X. Soil and water conservation effects of protective tillage measures on sloping farmland. *Sci. Soil Water Conser.* **2009**, *7*, 86–90. (In Chinese with English abstract).
29. Wei, Y.X.; Li, X.D.; Hu, T.T. Soil and water conservation and water-saving and soybean yield-increasing effects of different conservation tillage technology modes in slopping farmland. *J. NE. Agri. Uni.* **2013**, *44*, 51–55. (In Chinese with English abstract).
30. Tan, J.; Fan, H.M.; Xu, X.Q.; Jia, Y.F.; Wu, M. Comparison of practice values of soil and water conservation measures under the condition of snow melting and rainfall erosion. *Res. Soil Water Conser.* **2017**, *24*, 29–38. (In Chinese with English abstract).
31. Han, F.W.; Zhang, B.; Wang, Z.M.; Song, K.S.; Li, J.P. Study on the effect of soil erosion reduction corresponding to water and soil conservation measures in Jilin low mountain and mound area. *J. Jilin Agri. Uni.* **2007**, *29*, 668–672. (In Chinese with English abstract).
32. Li, F.; Li, X.G. The effect of different soil and water conservation tillage on runoff, sediment, and soil erosion. *J. Soil Water Conser.* **2022**, *5*, 142–146. (In Chinese with English abstract).
33. Zhang, S.L.; Zhang, X.Y.; Liu, X.B.; Liu, S.; Yu, T.Y. Tillage effect on soil erosion in typical black soil region. *J. Soil Water Conser.* **2009**, *23*, 11–15. (In Chinese with English abstract).
34. Zhang, X.Y.; Chen, Q.; Chen, Y.; Liu, S.; Li, X.F.; Li, H. Influence of no-tillage on soil and crop performance in the north cool region of Northeast China. *Sci. Agri. Sini.* **2013**, *46*, 2271–2277. (In Chinese with English abstract).
35. Shi, Y.L.; Chen, Y.S.; Liu, J.X.; Fan, H. The study of different tillage practices on soil and water conservation in black soil region of Northeast China. *Soil Water Conserv. China* **2019**, *1*, 47–49. (In Chinese with English abstract).
36. Wen, Y.H.; Wang, L.X.; Liu, T.J. Process of runoff and sediment generation on different slopes with ridged cropping in the black soil area of Northeast China. *Res. Soil Water Conser.* **2022**, *29*, 8–20. (In Chinese with English abstract).
37. Lv, G.; Ban, X.F.; Lei, Z.Y.; Wu, X.Y. Benefit of soil and water conservation in the process of harnessing a sloping farmland in the black soil region, Northeast China. *Sci. Soil Water Conser.* **2009**, *16*, 51–55. (In Chinese with English abstract).
38. Chen, G.; Fan, H.F.; Chen, H.S.; Dong, G.Q. Benefits of sediment reduction of soil conservation practices in the black soil region of Northeast China. *Sci. Soil Water Conser.* **2006**, *4*, 13–17. (In Chinese with English abstract).
39. Su, M.M.; Wang, X.J.; Gao, H.S. Effects of tillage measures and nitrogen fertilizers on surface runoff, soil erosion and inorganic nitrogen loss in sloping land of black soil region. *J. Soil Water Conser.* **2017**, *31*, 58–65. (In Chinese with English abstract).
40. Wang, B.T.; Ding, B.Q. The study of soil erosion protect tillage measures in the sloping land in the Northeast China. *Water Res. Hydr. NE.* **2008**, *26*, 64–66. (In Chinese with English abstract).
41. Ou, Y.L.; Xie, Y.J.; Ge, W.F.; Ju, M.R.; Chen, Y.Z. The water and soil conservation measures in the east and low mountains areas in the Heilongjiang. *Water Soil Conser. Tech.* **2018**, *6*, 8–10. (In Chinese with English abstract).
42. Gai, H.; Liu, P.Q.; Zhang, M.X.; Chen, B.X.; Wang, Y.C.; Wang, L.G. Effects of ridge planting on reducing runoff and soil organic carbon loss in black soil slope. *J. Soil Water Conser.* **2022**, *36*, 300–311. (In Chinese with English abstract).
43. Xu, X.H.; Sui, Y.Y.; Zhang, Y.; Wang, Y.F.; Liu, M.Y.; Liu, Y.J. Effects of different tillage on the soil and water conservation benefits in Northeast black soil area of China. *Sci. Soil Water Conser.* **2013**, *11*, 12–16. (In Chinese with English abstract).
44. Mou, Y.S.; Shen, H.O.; He, Y.F.; Li, C.L.; Guo, R.; Liu, D.M. Effects of ridge tillage patterns on soil erosion of sloping croplands in black soil region of Northeast China. *Bull. Soil Water Conser.* **2022**, *42*, 22–30. (In Chinese with English abstract).

45. He, Y.F.; Shen, H.O.; Zhang, Y.; Zhao, Z.J.; Mou, Y.S. Analysis of soil and water conservation effects of different straw returning patterns in sloping farmland in the Chinese black soil region. *J. Soil Water Conser.* **2020**, *34*, 89–94. (In Chinese with English abstract).
46. Niu, X.L.; Qin, F.C.; Yan, Z.Q.; Li, L.; Li, X.Q.; Liu, L.C. Efficacy of several tillage in conserving soil and water in slopping areas at the black soil in Northeast China. *J. Irr. Dra.* **2019**, *38*, 67–72. (In Chinese with English abstract).
47. Li, F.; Han, X.; Ma, X.L.; Wang, Y.J.; Song, T.Q.; Wang, Y.Y. Straw mulch controls runoff and nitrogen and phosphorus loss from slope farmland in black soil region of northeast China. *J. Soil Water Conser.* **2020**, *34*, 37–42. (In Chinese with English abstract).
48. Yang, Q.S.; Zhen, F.L.; Wen, L.L.; Gen, X.D.; An, J.; Wang, B. Effects of mulch cover on hillslope soil erosion and nutrient loss in black soil region of Northeast China. *Bull. Soil Water Conser.* **2011**, *31*, 1–5. (In Chinese with English abstract).
49. Cao, Y.S.; Li, H.P.; Xiao, B. Effect of straw mulching on soil and water loss under different soil bulk densities on slope cropland in black soil region. *Bull. Soil Water Conser.* **2021**, *41*, 56–61. (In Chinese with English abstract).
50. He, C.; Wang, L.; Zhen, F.L.; He, X.; Fu, H. Effects of ridge tillage on hillslope soil erosion in Thin layer black soil region. *J. Soil Water Conser.* **2018**, *32*, 24–28. (In Chinese with English abstract).
51. Chen, Y.; Zhang, Y.Y.; Li, S.X. Comparative study on conservational tillage in slope and flat farmland. *Sys. Sci. Comp. Stu. Agri.* **2011**, *27*, 485–489. (In Chinese with English abstract).
52. Sui, Y.Y.; Ou, Y.; Yan, B.X.; Xu, X.H.; Rousseau, A.N.; Zhang, Y. Assessment of micro-basin tillage as a soil and water conservation practice in the black soil region of Northeast China. *PLoS ONE* **2016**, *11*, 1–16. (In Chinese with English abstract). [CrossRef] [PubMed]
53. Chai, Y.; Wei, Y.X.; Zhang, B.L.; Bai, Y. Impacts of slopping farm land management measures and their combination on soil and water environment and nutrient loss. *Agri. Mech. Stu.* **2015**, *1*, 177–182. (In Chinese with English abstract).
54. Chen, Q.; Yuriy, S.K.; Chen, Y.; Li, X.F.; Li, H.; Song, C.Y.; Zhang, X.Y. Seasonal variations of soil structures and hydraulic conductivities and their effects on soil and water conservation under no-tillage and reduced tillage. *Acta Pedologica Sinica* **2015**, *51*, 11–21. (In Chinese with English abstract).
55. Yang, S.Q.; Xin, L.; Liu, H.Y.; Han, R.Y.; Yan, L.Z. Effect of planting patterns on soil nitrogen and phosphorus loss in slope farmland in the main Songhua river basin. *J. NW Uni.* **2018**, *46*, 61–69. (In Chinese with English abstract).
56. Mou, T.S.; Shen, H.O.; Wang, D.L.; Zhang, Y.; Wu, J.L.; Huang, Z.Y. Effects of crushed corn straw returning on soil erosion characteristics at the black soil hillslopes. *J. Soil Water Conser.* **2022**, *36*, 78–91. (In Chinese with English abstract).
57. Zhang, X.Y.; Li, J.Y.; Guo, M.J.; Hu, W.; Li, J.Y. Effects of straw mulching and no tillage for continuous 14 years on soil and water conservation in mollisols sloping farmland. *J. Soil Water Conser.* **2022**, *36*, 44–50. (In Chinese with English abstract).
58. Xu, X.M.; Zhang, F.L.; Wilson, G.V.; He, C.; Lu, J.; Bian, F. Comparison of runoff and soil loss in different tillage systems in the Mollisol region of Northeast China. *Soil Till. Res.* **2018**, *177*, 1–11. [CrossRef]
59. Chen, S.; Burras, C.L.; Li, L.E.; Zhang, X.Y. Interrelationship among slope steepness, tillage practice and rainfall properties with surface runoff and soil loss on Mollisols in Northeast China. *Arch. Agron. Soil Sci.* **2019**, *65*, 1860–1872. [CrossRef]
60. Yang, X.M.; Zhang, X.P.; Deng, W.; Fang, H.J. Black soil degradation by rainfall erosion in Jilin, China. *Land Degra. Deve.* **2003**, *14*, 409–420. [CrossRef]
61. Li, H.L.; Shen, H.O.; Wang, Y.; Wang, Y.; Gao, Q. Effect of ridge tillage and straw returning on runoff and soil loss under simulated rainfall in the Mollisol region of Northeast China. *Sustainability* **2021**, *13*, 10614. [CrossRef]
62. Dai, T.Y.; Wang, L.Q.; Li, T.N.; Qiu, P.P.; Wang, J. Study on the characteristics of soil erosion in the black soil area of Northeast China under natural rainfall conditions: The case of Sunjiagou small watershed. *Sustainability* **2022**, *14*, 8284. [CrossRef]
63. Zhang, Y.J. Effects of conservation tillage on soil and water loss from sloping farmland in Heibeishan watershed. *Bull. Soil Water Conser.* **2012**, *32*, 103–105. (In Chinese with English abstract).
64. Jiang, B.W.; Zhao, S.D.; Dan, W.; Jin, L.; Li, Y.M.; Guo, W.Y.; Xu, M.; Zhang, Z. Effect of slope and tillage measures on soil erosion and yield of soybean. *Soyb. Sci.* **2015**, *34*, 238–242. (In Chinese with English abstract).
65. Yang, A.M.; Shen, C.P.; Liu, F.; Yin, J.F.; Den, Y.J. Study on soil and water conservation benefit of contour check in sloping field. *J. Soil Water Conser.* **1994**, *8*, 52–58. (In Chinese with English abstract).
66. Yang, R.C. Monitoring study on wind erosion in Hailun of the typical Mollisols farmland in Northeast China. Master's Thesis, Northeast Agricultural University, Harbin, China, 2018. (In Chinese with English abstract).
67. Chu, Z.D.; Xie, R.Z.; Li, S.K.; Wang, K.R.; Liu, W.R.; Zhang, J.Y. Spring corn conservation tillage effects of the ageing resistant film mulch and the alternative fallow remaining high stubble in Northeast of China. *J. Mai. Sci.* **2018**, *18*, 70–72. (In Chinese with English abstract).
68. Wang, Y.; Yan, M.Y.; Liu, P.L. Contribution partition of water and wind erosion on cultivated slopes in northeast black soil region of China. *J. Nuc. Agri. Sci.* **2010**, *24*, 790–795. (In Chinese with English abstract).
69. Tuo, D.B.; Duan, Y.; Zhao, P.Y.; Zheng, D.W.; Chen, M.; Zhao, J. Ecological effect of intercropping strips keeping stubble on preventing field from wind erosion in dryland farming areas. *Acta Agri. Bore. Sini.* **2002**, *17*, 63–67. (In Chinese with English abstract).
70. Li, S.L.; Li, H.P.; Lin, Y.; Xiao, B.; Wang, G.P. Effects of tillage methods on wind erosion in farmland of Northeast China. *J. Soil Water Conser.* **2019**, *33*, 110–118. (In Chinese with English abstract).
71. Zhao, J.; Zhang, L.F.; Liu, J.H.; Li, M. Effect of conservation tillage on soil moisture and wind blow mass. *J. Anhui Agri. Sci.* **2010**, *38*, 4720–4728. (In Chinese with English abstract).

72. Wang, G. Conservation tillage with standing corn residue and its corresponding corn harvester. Phd Thesis, Jilin University, Changchun, China, 2016. (In Chinese with English abstract).
73. Cui, X. The critical technic of conservation tillage in the Liao River conservational region. *Agri. Sci. Tech. Equip.* **2015**, *04*, 7–12. (In Chinese with English abstract).
74. Lv, Z.C. Effect of Liaoning Northwest different agricultural measures on soil erosion sowing. *Jilin Water Technic.* **2015**, *10*, 24–26. (In Chinese with English abstract).
75. Qin, H.L.; Gao, W.S.; Ma, Y.C.; Zhao, P.Y. Effect of standing crop stubble on soil erosion by wind under no-tillage. *Tran. CSAE.* **2008**, *24*, 66–71. (In Chinese with English abstract).
76. Chang, X.H.; Zhao, G.C.; Zhang, W.; Hou, L.B.; Meng, X.Y.; Yuan, B.L. Effect of crop stubble mulch on farmland wind erosion. *J. Soil Water Conser.* **2005**, *19*, 28–30. (In Chinese with English abstract).
77. Borrelli, P.; Panagos, P.; Alewell, C.; Ballabio, C.; de Oliveira Fagundes, H.; Haregeweyn, N.; Lugato, E.; Maerker, M.; Poesen, J.; Vanmaercke, M.; et al. Policy implications of multiple concurrent soil erosion processes in European farmland. *Nat. Sustain.* **2022**, *6*, 103–112. [CrossRef]
78. Zhang, W.B.; Xie, Y.; Liu, B.Y. Rainfall erosivity estimation using daily rainfall amounts. *Sci. Geogr. Sin.* **2002**, *22*, 705–711. (In Chinese with English abstract).
79. Li, J.; Yu, W.; Du, J.; Song, K.; Xiang, X.; Liu, H.; Zhang, Y.; Zhang, W.; Zheng, Z.; Wang, Y.; et al. Mapping Maize Tillage Practices over the Songnen Plain in Northeast China Using GEE Cloud Platform. *Remote Sens.* **2023**, *15*, 1461. [CrossRef]
80. Scheper, S.; Weninger, T.; Kitzler, B.; Lackóová, L.; Cornelis, W.; Strauss, P.; Michel, K. Comparison of the Spatial Wind Erosion Patterns of Erosion Risk Mapping and Quantitative Modeling in Eastern Austria. *Land* **2021**, *10*, 974. [CrossRef]
81. Wang, Y.; Zhang, Z.; Guo, Z.; Chen, Y.; Yang, J.; Peng, X. In-situ measuring and predicting dynamics of soil bulk density in a non-rigid soil as affected by tillage practices: Effects of soil subsidence and shrinkage. *Soil Tillage Res.* **2023**, *234*, 105818. [CrossRef]
82. Zhang, X.; Zhang, W.C.; Wu, W.; Liu, H.B. Horizontal and vertical variation of soil clay content and its controlling factors in China. *Sci. Total Environ.* **2023**, *864*, 161141. [CrossRef]
83. Wang, X.; Zhao, X.; Zhang, Z.; Yi, L.; Zuo, L.; Wen, Q.; Liu, F.; Xu, J.; Hu, S.; Liu, B. Assessment of soil erosion change and its relationships with land use/cover change in China from the end of the 1980s to 2010. *Catena* **2016**, *137*, 256–268. [CrossRef]
84. Wang, B.; Zhao, X.; Wang, X.; Zhang, Z.; Yi, L.; Hu, S. Spatial and temporal variability of soil erosion in the black soil region of Northeast China from 2000 to 2015. *Environ. Monit. Assess.* **2020**, *192*, 370. [CrossRef] [PubMed]
85. Shen, Y.; Gu, J.; Liu, G.; Wang, X.; Shi, H.; Shu, C.; Zhang, Q.; Guo, Z.; Zhang, Y. Predicting soil erosion and deposition on sloping farmland with different shapes in northeast China by using 137 Cs. *Catena* **2023**, *229*, 107238. [CrossRef]
86. Ryken, N.; Vanden Nest, T.; Al-Barri, B.; Blake, W.; Taylor, A.; Bodé, S.; Ruysschaert, G.; Boeckx, P.; Verdoodt, A. Soil erosion rates under different tillage practices in central Belgium: New perspectives from a combined approach of rainfall simulations and 7 Be measurements. *Soil Tillage Res.* **2018**, *179*, 29–37. [CrossRef]
87. Zhang, X.C.J. Cropping and Tillage Systems Effects on Soil Erosion under Climate Change in Oklahoma. *Soil Sci. Soc. Am. J.* **2012**, *76*, 1789–1797. [CrossRef]
88. Bhatt, R.; Khera, K.L. Effect of tillage and mode of straw mulch application on soil erosion in the submontaneous tract of Punjab, India. *Soil Tillage Res.* **2006**, *88*, 107–115. [CrossRef]
89. Pei, L.; Wang, C.; Sun, L.; Wang, L. Temporal and Spatial Variation (2001–2020) Characteristics of Wind Speed in the Water Erosion Area of the Typical Black Soil Region, Northeast China. *Int. J. Environ. Res. Public Health* **2022**, *19*, 10473. [CrossRef] [PubMed]
90. Xu, S.; Fu, Q.; Li, T.; Meng, F.; Liu, D.; Hou, R.; Li, M.; Li, Q. Spatiotemporal characteristics of the soil freeze-thaw state and its variation under different land use types—A case study in Northeast China. *Agric. For. Meteorol.* **2022**, *312*, 108737. [CrossRef]
91. Liu, G.; Qu, M.; Feng, G.; Chu, Q.; Cao, J.; Yang, J.; Cao, L.; Feng, Y. Application study of monthly precipitation forecast in Northeast China based on the cold vortex persistence activity index. *Theor. Appl. Climatol.* **2018**, *135*, 1079–1090. [CrossRef]
92. Ellison, W.D. Soil Erosion by Rainstorms. *Science* **1950**, *111*, 245–249. [CrossRef]
93. Chalise, D.; Kumar, L.; Sharma, R.; Kristiansen, P. Assessing the Impacts of Tillage and Mulch on Soil Erosion and Corn Yield. *Agronomy* **2020**, *10*, 63. [CrossRef]
94. Dong, Y.; Xuan, F.; Huang, X.; Li, Z.; Su, W.; Huang, J.; Li, X.; Tao, W.; Liu, H.; Chen, J. A 30-m annual corn residue coverage dataset from 2013 to 2021 in Northeast China. *Sci. Data* **2024**, *11*, 216. [CrossRef] [PubMed]
95. Li, R.; Zheng, J.; Xie, R.; Ming, B.; Peng, X.; Luo, Y.; Zheng, H.; Sui, P.; Wang, K.; Hou, P.; et al. Potential mechanisms of maize yield reduction under short-term no-tillage combined with residue coverage in the semi-humid region of Northeast China. *Soil Tillage Res.* **2022**, *217*, 105289. [CrossRef]
96. Jiang, F.; Qian, Y.; Guo, Z.; Gao, L.; Zhang, Z.; Cao, Z.; Guo, J.; Liu, F.; Peng, X. Evaluating the regional suitability of conservation tillage and deep tillage based on crop yield in the black soil of Northeast China: A meta-analysis. *Acta Pedol. Sin.* **2022**, *59*, 935–952. (In Chinese with English abstract).